Stepwise Collapse of Monolayers of Cyclolinear Poly(organosiloxane)s at the Air/Water Interface: A Brewster-Angle Microscopy and Scanning Force Microscopy Study

A. I. Buzin,[†] Yu. K. Godovsky,[‡] N. N. Makarova,[§] J. Fang,[∥] X. Wang,[⊥] and C. M. Knobler*,[⊥]

Institute of Synthetic Polymer Materials, Russian Academy of Sciences, 70 Profsoyuznaya ul., 117393 Moscow, Russia, Karpov Institute of Physical Chemistry, 10 Vorontsovo Pole ul., 103064 Moscow, Russia, Nesmeyanov Institute of Organo-Element Compounds, Russian Academy of Sciences, 28 Vavilova ul., 117813 Moscow, Russia, Center for Biomolecular Science and Engineering, Naval Research Laboratory, Washington, D.C. 20375-5438, and Department of Chemistry and Biochemistry, University of California, Los Angeles, California 90095-1569

Received: July 30, 1999; In Final Form: October 9, 1999

We report studies of the collapse of monolayers of cyclolinear poly(organosiloxane)s that consist of six-membered rings joined by oxygen bridges and that contain two phenyl groups per monomer unit. Surface pressure−area isotherms show that these films undergo a stepwise collapse. The organization within the films has been examined at different stages of the collapse process by Brewster-angle microscopy. Films transferred to mica by the Langmuir−Blodgett technique have been imaged by scanning force microscopy. Five fractions of an atactic polymer with molecular weights (M_W) ranging from 8900 to 85 000 and one trans-tactic polymer ($M_W = 8100$) have been investigated. Bilayers of the fractions with the highest M_W's appear in the form of islands but the bilayers in the other samples have the form of ribbons 50−250 nm wide.

Introduction

It has long been known that amphiphilic polymers can be spread as monolayers at the air/water interface, and many surface pressure−area isotherm studies of polymer monolayers have been reported.[1] Although the organization of the polymer on the water surface may be inferred from these thermodynamic investigations, it was not until the advent of imaging techniques such as Brewster-angle microscopy (BAM)[2,3] that monolayers could be examined directly. In the first of such experiments on polymers, which are now commonplace, monolayers of poly(dimethylsiloxane) (PDMS) were studied by Mann et al.,[4] who were able to see coexistence between high- and low-density polymer phases. The optical resolution in such studies is 2−3 μm at best. Smaller features can be imaged by transferring the monolayers to solid supports by the Langmuir−Blodgett (LB) technique and examining their morphology by transmission electron microscopy[5] or scanning force microscopy (SFM).[6]

The imaging methods have been employed to advantage in investigations of collapse, the process by which monolayers undergo a transition to the bulk phase. A monolayer is often studied at surface pressures in excess of the equilibrium spreading pressure (ESP), the pressure at which it is in equilibrium with the bulk phase. Under these conditions, it is metastable with respect to the bulk. As the surface pressure is increased beyond the ESP, the stability of the monolayer decreases. It is usually observed that bulk phase begins to form rapidly at a threshold pressure called the collapse pressure, at which point the surface pressure drops to the ESP. But in some cases monolayers collapse by the successive formation of layers. Such stepwise collapse is marked by a series of plateaus in the isotherm, each of which is associated with a discrete layer.

Stepwise collapse has been observed in isotherms of monolayers of liquid crystals[7,9] and the nature of the multilayers has been determined by ellipsometry[9] and BAM[10,11] and by SFM measurements on LB films.[12] By linking a mesogenic cyanobiphenyl to a siloxane, Ibn-Elhaj et al.[13,14] were able to obtain collapse into bilayers and trilayers, which they examined by BAM and X-ray reflectivity.

The formation of multilayers appears to be common in siloxane polymers. BAM images of PDMS[4] show evidence of bilayer formation at collapse and bilayers have also been observed in BAM images of carbosilane dendrimers.[15] Isotherms of cyclolinear poly(organosiloxane)s (CLPOS) are remarkable in that as many as seven distinct plateaus can be observed on collapse.[16,17] An investigation by SFM of LB films formed from these polymers[18] showed that the bilayer appears in the form of monolayer ribbons about 50 nm wide and several 100 μm long. As the film is compressed across the monolayer−bilayer plateau, the number of ribbons increases but their width remains constant.

The present study is part of an effort to understand the mechanism of collapse and to determine the factors that affect the morphology of the multilayers formed. It has been observed in previous studies of CLPOS[19,20] that the isotherms are strongly affected by the molecular weight and molecular structure of the polymer. We have therefore undertaken BAM and SFM studies of monolayers and multilayers formed by a series of CLPOS with different molecular weights and tacticities.

Experimental Section

We have studied a representative series of fractions of cyclolinear poly(organosiloxane)s that consist of six-membered rings joined by oxygen bridges and that contain two phenyl groups per monomer unit (PMPhCS-6). The synthesis of these

[†] Institute of Synthetic Polymer Materials, Russian Academy of Sciences.
[‡] Karpov Institute of Physical Chemistry.
[§] Nesmeyanov Institute of Organo-Element Compounds, Russian Academy of Sciences.
[∥] Naval Research Laboratory.
[⊥] University of California, Los Angeles.

10.1021/jp992708+ CCC: $18.00
Published on Web 12/03/1999

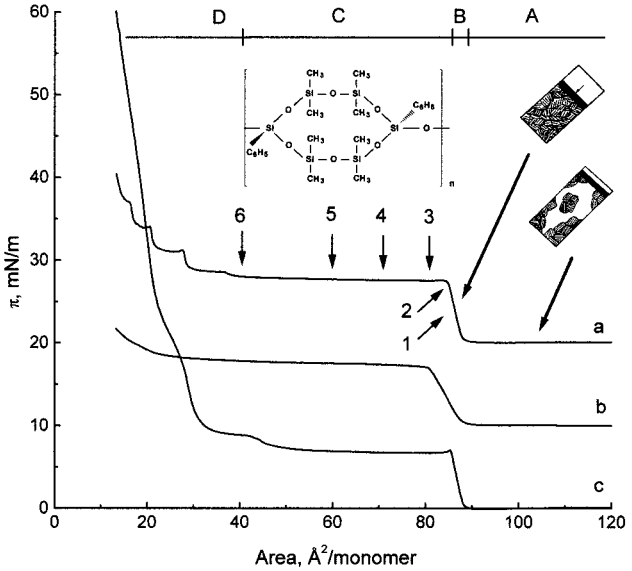

Figure 1. Surface pressure−surface area isotherms at 24 °C. (a) Fraction II. The isotherm is typical of all other atactic samples. (b) Fraction I. (c) Trans-tactic fraction TR. Isotherm a has been displaced upward by 20 mN m^{-1} and isotherm b by 10 mN m^{-1}. The molecular structure of trans-tactic PMPhCS-6 is shown in the inset.

TABLE 1: Characteristics of the Polymers Investigated

	tacticity	$[\eta]$, dL g^{-1}	M_W	$\bar{x}_n$	T_M, °C	T_i, °C
I	atactic	0.06	8900	16	51	350
II	atactic	0.14	19200	35	47	408
III	atactic	0.20	28500	52	45	410
IV	atactic	0.33	49000	90	42	421
V	atactic	0.55	85000	154	41	432
TR	trans-tactic	0.05	8100	15	145	425

polymers has been described in detail.[21] The samples differ in their molecular weight and tacticity, which in this case is the ordering of the phenyl substituents at silsesquioxane silicon atoms atoms (silicon atoms connected to three oxygens). The molecular structure of the monomer unit of the trans-tactic polymer is shown in the inset in Figure 1. In this case the phenyl substituents at the silsesquioxane silicons are located on opposite sides of the monomer ring; they are randomly oriented in the atactic polymer. Detailed surface pressure−area isotherms for this series of polymers have been reported elsewhere.[20,21] The characteristic viscosity η, weight-average molecular weight M_W, and weight-average degree of polymerization $\bar{x}_n$ are summarized in Table 1. These polymers melt to a columnar liquid-crystalline phase, which undergoes a transition to an isotropic phase at higher temperature. Melting temperatures, T_M, and isotropization temperatures, T_i, are also given in the table. The temperatures were measured in quenched samples by polarization microscopy in a nitrogen atmosphere at a heating rate of 10 K min^{-1}.

Langmuir films were prepared on a Nima Type 611 trough made of poly(tetrafluoroethylene) and the surface pressure was measured with a filter-paper Wilhelmy plate. The polymers were spread from 0.2 mg mL^{-1} chloroform and toluene solutions (both Fisher spectranalyzed) on Milli-Q water (18 MΩ, pH 5.7) at a constant temperature of about 24 °C. LB films were deposited on freshly cleaved mica by vertical dipping at constant surface pressure. The dipping speed was 0.5 mm min^{-1}.

Topographic atomic-force microscopy (AFM) and lateral force microscopy (LFM) images of transferred layers were obtained in contact mode with a Park AutoProbe CP scanning force microscope using a 100 μm scanner. Triangular Si_3N_4 cantilevers with a normal spring constant of 0.05 N m^{-1} (Park Scientific Instruments) were employed, and the force was kept below 1 nN. All SFM images shown in this paper have been flattened but have not undergone any other treatment. The Brewster-angle microscope, which was used to image the films on the water surface, has been already described in detail.[22]

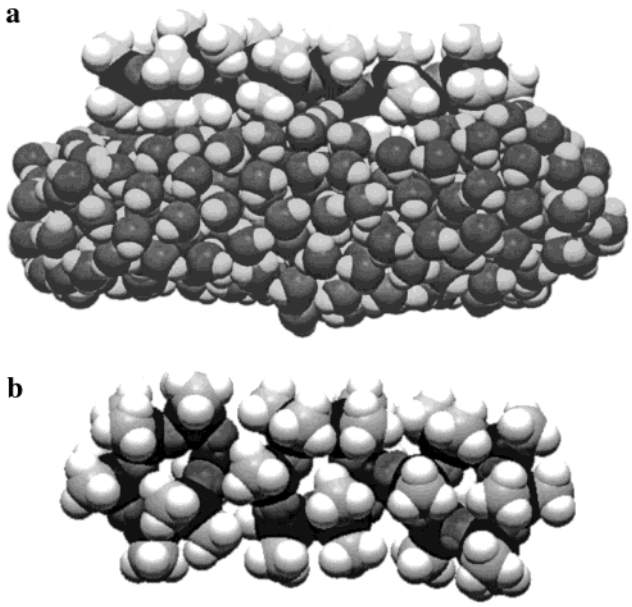

Figure 2. Calculated conformation for a methyl-substituted trimer on a water cluster: (a) side view; (b) top view. For clarity, the underlying slab of water is not shown.

Results

Surface Pressure−Area Isotherms. Extensive isotherm studies of films of PMPhCS-6 polymers that differ in molecular weight and molecular structure have recently been reported.[19] We review these results here in order to place our measurements in context; all of the isotherms that we have measured are consistent with this study. All the polymers investigated can be spread from solution onto the water surface; parts a−c of Figure 1 show three characteristic $\pi-A$ isotherms at 24 °C. In region A, the surface pressure is immeasurably low. It rises linearly at the completion of a monolayer, region B, in all three cases at a monomer area of about 90 Å^2. Cyclic polysiloxanes with methyl groups as the substituents at the silsesquioxane silicons have been reported[16,23] to have monolayer areas of 108 and 93 Å^2. (In an earlier paper[18] we reported a value of 130 Å^2, but this area was computed with an erroneous value for the molecular weight of the monomer and should have been given as 103 Å^2.)

To shed light on the differences in monolayer areas between the phenyl- and methyl-substituted polymers, we have investigated the structures by molecular modeling using the program Macromodel[24] with the MM2* force field.[25] For computational simplicity, we examined the conformations of trimers using a Monte Carlo search technique. The optimal conformation of an isolated trimer was twisted with the plane of the central ring roughly perpendicular to that of the other rings. To include the effect of the water subphase, we added a slab of 992 water molecules, whose initial configuration was that determined by Jorgensen et al.[26] After inclusion of the water, a search of 300 conformers led to a stable geometry for the methyl trimer in which the molecule lies essentially flat on the water surface, Figure 2a. In this conformation, all 10 methyls in a monomer are in equatorial positions with respect to the ring; six above

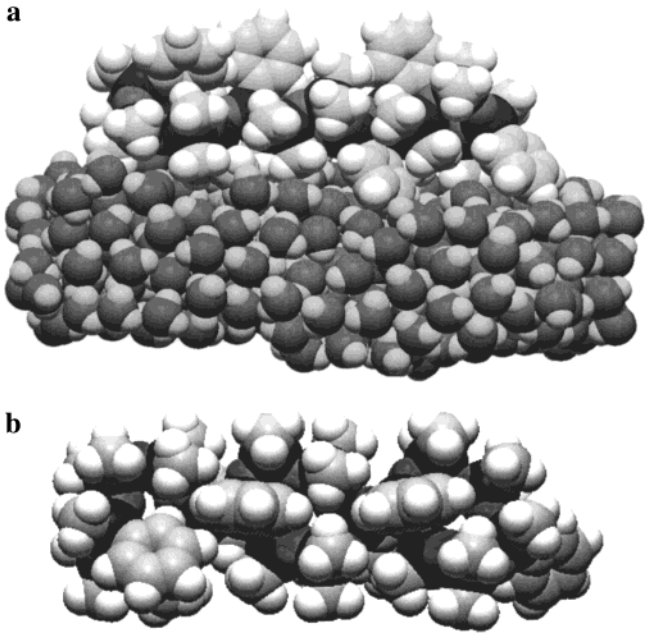

Figure 3. Calculated conformation for a trans-tactic phenyl-substituted trimer on a water cluster: (a) side view; (b) top view. For clarity, the underlying slab of water is not shown.

the plane and four below. Thus, the simple picture in which all of the methyls lie above the ring is probably incorrect, although the oxygens are in contact with water molecules as had been supposed. When the molecule is viewed from above, Figure 2b, one finds that, measured from the extremes of the H atoms, the trimer is about 26.2 Å long and 10.2 Å wide, which corresponds to an area per monomer of 89 $Å^2$; the area would be somewhat greater in a polymer because the outer rings in the trimer are not as flat as the middle one. This area is markedly smaller than that computed earlier.[18] In that case, however, the structure was one in which all the methyl groups were placed above the plane, there was no water present and no search for a conformational minimum was carried out. The computed height of the trimer is 6.2 Å, which can be compared with the value 7.5 Å found in AFM measurements for the height of a monolayer transferred to mica.[18]

We have also carried out a conformational analysis for a trimer segment of the trans-tactic polymer, and the results of the conformational search with the MM2* force field are shown in Figure 3. Here the phenyl groups above the ring are axial and, as shown in Figure 3b, they are aligned. The phenyl groups below the ring have pseudoequatorial positions. The trimer is about 28 Å long and 10 Å wide, corresponding to an area of 93 $Å^2$ per monomer. The computed thickness of the monlayer is 10.9 Å, which is consistent with AFM measurements of transferred films (see below). The contact angle of water on monolayer LB films of the phenyl-substituted polymer on mica is 89 ± 3°, which would be expected with an orientation in which the hydrophobic portions of the molecule point toward the air. A similar result was obtained for the methyl-substituted polymer.[18]

The conformational analyses give an area per molecule for the trans-tactic phenyl-substituted polymer slightly larger than that of the polymer with methyl substituents, while the isotherm measurements, though scattered, give consistently larger areas for the methyl-substituted polymer. This is probably indicative of more regular packing of the trans-tactic polymer on the water surface, which, as will be shown, is consistent with BAM studies of the monolayer and SFM measurements of the organization of the collapsed films.

The isotherms show a plateau corresponding to the formation of a bilayer upon compression beyond the monolayer, region C. In atactic samples, the height of the plateau is 7.5 mN m^{-1} and is essentially independent of molecular weight. A slightly lower plateau, 6.7 mN m^{-1}, is found for the trans-tactic polymer. In general, further compression leads to several steps and plateaus in the surface pressure, region D, at monomer areas that are approximately $^1/_2$, $^1/_3$, $^1/_4$, $^1/_5$, $^1/_6$ that of the monolayer. Each increase in the surface pressure therefore corresponds to formation of a complete *n*-layer ($n = 2-6$). The sharpness of the steps increases with increasing molecular weight and for $n > 2$ the step height decreases approximately with M_W^{-1} and converges to $\Delta\pi = 0$ at about $M_W = 8000$. (This dependence on molecular weight probably accounts for the lack of distinct steps beyond the first in the isotherms of actactic fraction I,[19] for which $M_W = 8900$). In contrast, Granick et al.[27] have reported that the plateau pressures in mixtures of cyclic PDMS polymers of different ring sizes increase with molecular weight.

The isotherm for the trans-tactic fraction TR exhibits two large steps that correspond to the formation of a bilayer and trilayer. Their height exceeds that for fraction II by a factor of 3, but the area ratios are the same. Compression beyond the trilayer leads to a very steep stepless increase in the surface pressure, which is associated with the formation of a thick layer.[19]

All of the isotherms studied do not correspond to equilibrium at densities above that of a monolayer. If the compression is stopped, the surface pressure falls to the ESP. It drops further upon reexpansion but rises to the ESP when the barrier is stopped. Similar behavior is observed in smectic ferroelectrics[7,8] and liquid-crystalline-side-chain polymers.[28] The ESP for the atactic polymers is 6.7 mN m^{-1}, and that for the transtactic polymer is 6.0 mN m^{-1}.

Brewster-Angle Microscopy. BAM images obtained at low density show that the monolayer exists in the form of islands of a condensed phase separated by regions of very low concentration. This coexistence is evident in an image of fraction V, Figure 4a. The distance between islands decreases with compression in region A, and the onset of a measurable surface pressure corresponds to the point at which the islands have just coalesced. The bright line in Figure 4a is a boundary between islands that have just come into contact and coalesced under compression. On decompression the dense monolayer breaks up into irregularly shaped regions.

SFM images of transferred monolayers of the methyl-substituted polymers show a structure in which there is a parallel alignment of extended chains,[18] and a similar organization would be expected for the phenyl-substituted polymers. The BAM images of a dense monolayer should show a mosaic structure consisting of domains that differ in the orientation of the molecular axes; our BAM measurements are consistent with this picture. As shown in an image of a condensed monolayer of fraction II, Figure 4b, the reflectivity within the condensed film is not uniform. The contrast in the texture changes with the orientation of the analyzer, which shows that it is associated with molecular anisotropy. This is consistent with a model in which there are regions of the monolayer with different orientations of extended aligned polymers. The greatest anisotropy is observed in images of the trans-tactic polymer, Figure 4c,d. These anisotropic domains are typically lamellar and are often oriented perpendicular to island boundaries, as shown in Figure 4c.

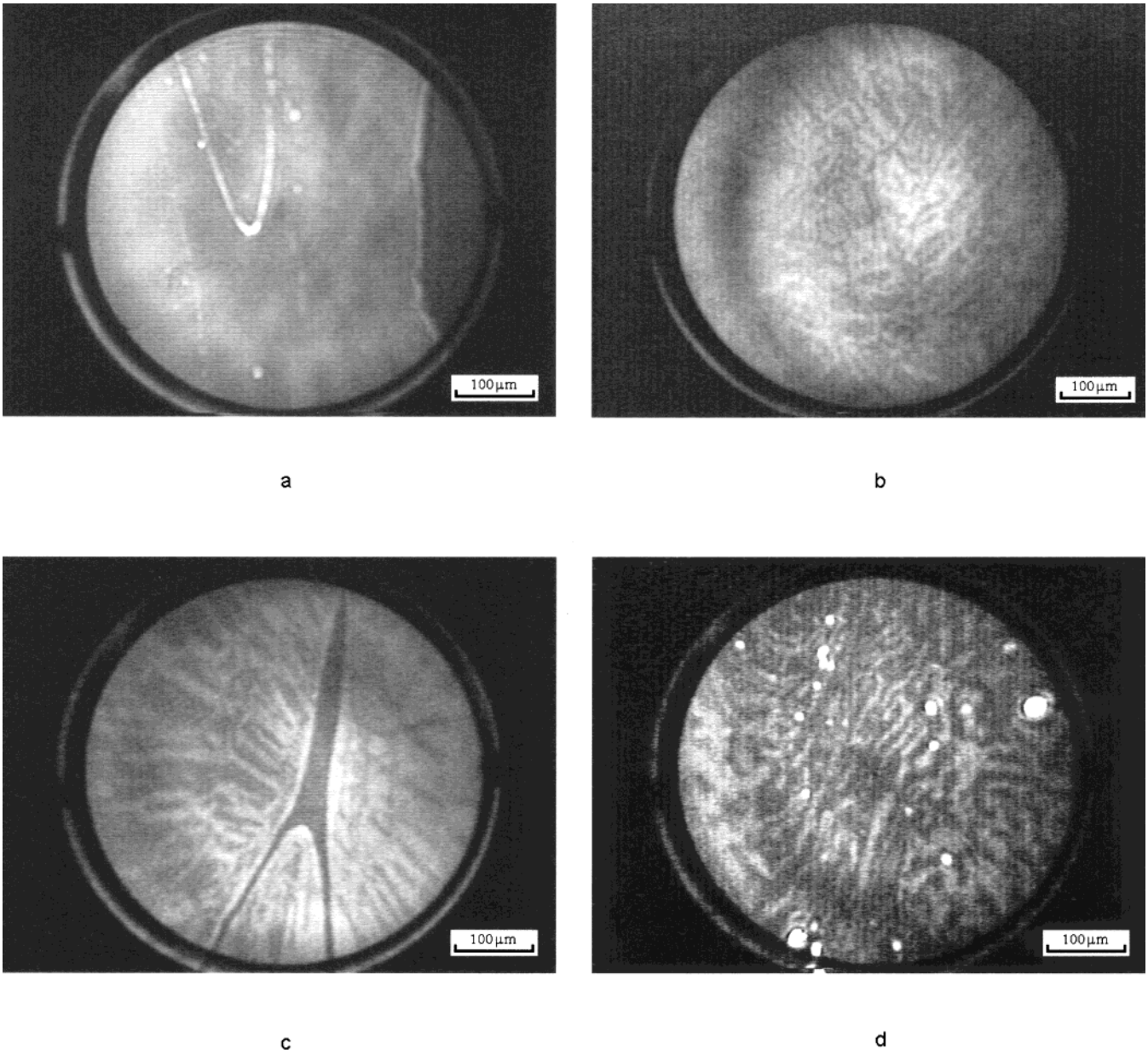

Figure 4. Brewster angle microscopy images of monolayers at the air/water interface in region A at 24 °C: (a) fraction V; (b) fraction II; (c) fraction TR, showing domain boundary; (d) fraction TR.

Figure 5 shows gradual growth of the bilayer of the trans-tactic fraction in the plateau region C. The second layer appears initially as isolated bright spots, but with further compression it evolves into a more lamellar pattern. Although the texture in the underlying monolayer changed with the rotation of the analyzer, there was no obvious anisotropy in the texture of the bilayer. The bilayers in low-molecular-weight atactic fractions grow in a similar fashion. Different textures are observed for the fraction with the highest molecular weight. The bilayer appears in the form of wide bands about 1 mm in length and 10 μm wide, Figure 5d. The density of bands increases as the film is compressed until the entire surface is covered by the bilayer.

The formation of a trilayer can be observed upon further compression, but it begins to collapse as soon as the compression is stopped. Several consecutive BAM images made during decompression of the trilayer of the trans-tactic fraction are shown in Figure 6. The surface layer fractures into islands of the multilayer separated by the monolayer. Similar results were found previously for the methyl-substituted polymer.[18]

Scanning Probe Microscopy. The mechanism of monolayer collapse was investigated by transferring monolayers and multilayers onto mica during the collapse process. Transfers were accomplished by vertical dipping at constant speed and constant surface pressure. In the usual Langmuir−Blodgett procedure, a constant pressure is maintained by decreasing the area of the monolayer to compensate for the material deposited on the substrate. This can be done only for transfers from regions in which the surface pressure increases with a decrease in area, which is not the case where the isotherm exhibits a plateau. To circumvent this problem, the monolayer was compressed at a constant speed until the transfer point in the bilayer plateau. The compression was then stopped and the surface pressure dropped. The surface pressure would then increase on compression and a constant pressure could be maintained at 0.3−0.5 mN m^{-1} below the dynamic surface pressure of the plateau during the transfer. With this method we obtained reasonable

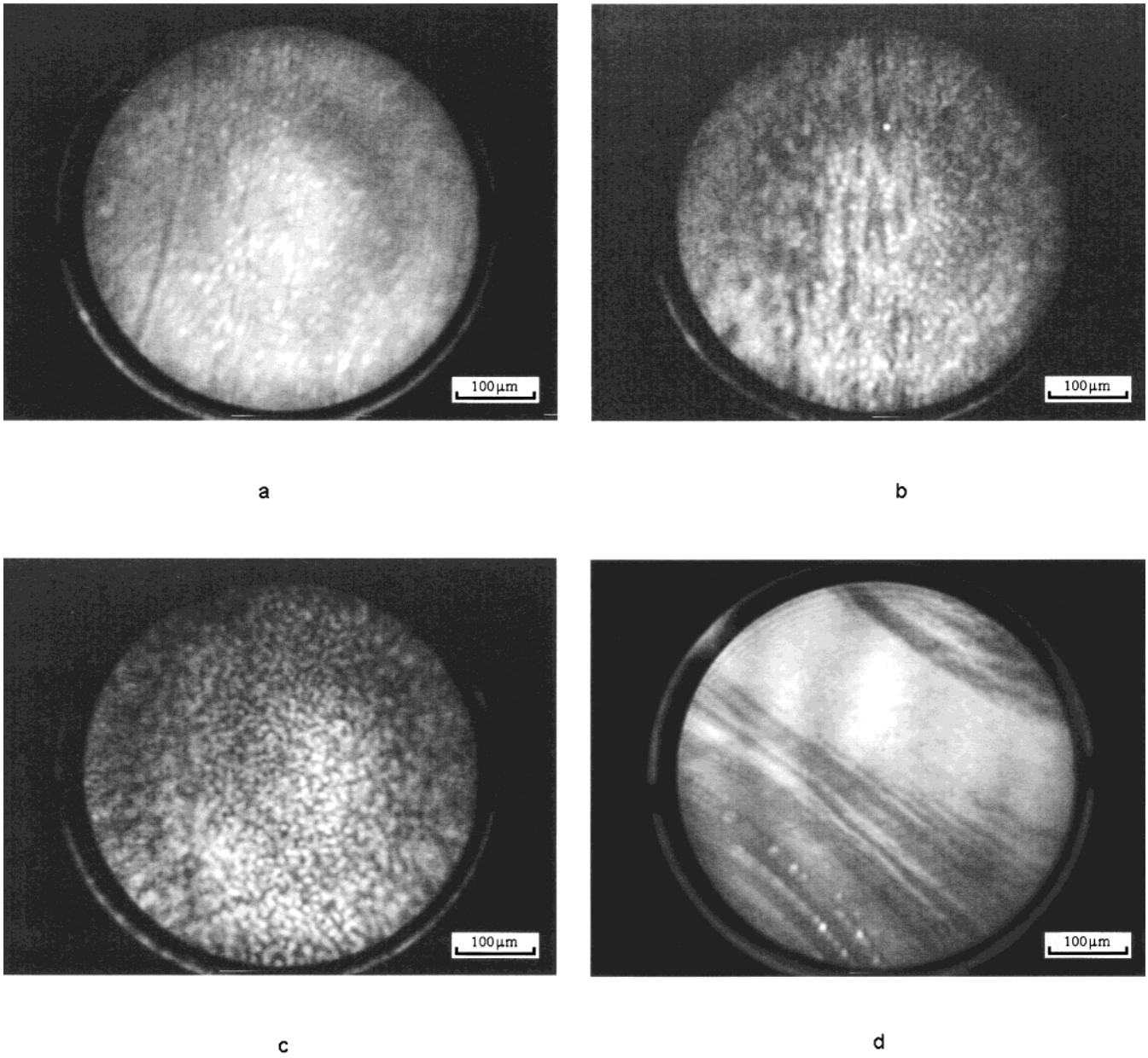

Figure 5. BAM images from the monolayer−bilayer transition region C at 24 °C: (a) fraction TR, point 3 on the isotherm; (b) fraction TR, point 4; (c) fraction TR, point 5; (d) fraction V, point 5.

transfer ratios of 1.3 ± 0.3. Transfers have also been made at the equilibrium spreading pressure; they exhibit surface structures similar to those found in the more controlled transfers.

Dense monolayers transferred from point 1 are quite uniform with very few defects. The thickness of the monolayer measured in contact mode was 1.0−1.2 nm, in agreement with the layer thickness obtained previously[18] and the 1.09 nm estimate from the molecular modeling. The layer thickness calculated from the area of the monolayer coverage assuming the density of the polymer to be 1 g cm^{-3} is 1.05 nm.

Transfers made from the region where the monolayer and bilayer coexist show the second layer clearly on top of the dense monolayer. In the atactic fractions of intermediate molecular weight (M_W = 19 200, 28 500), the second layer appears in the form of ribbons of nearly equal width of 200−250 nm. The thickness of the ribbons corresponds to that of the monolayer. On compression, the width of the ribbons remains constant, but the surface coverage increases in proportion to the degree of compression (Figure 7a,b). At the end of the monolayer−bilayer transition almost all the surface is covered by the ribbons (Figure 7c).

Ribbons also appear in the second layer of the low-molecular-weight (M_W = 8900) atactic fraction (Figure 8a), but they aggregate with further compression. The growth of the bilayer is different with the high-molecular-weight (M_W = 49 000, 85 000) atactic fractions. The surface of the transferred samples is quite inhomogeneous. BAM images of these fractions on the water surface show this behavior as well. The second layer appears in the form of elongated islands whose size increases with compression (Figure 8b).

The early stages of the collapse process for the low- and intermediate-molecular-weight atactic fractions have been examined in transfers made from the monolayer at the collapse point (point 2) at surface pressures above the equilibrium spreading pressure. In these experiments we used the method of time-resolved transfer[18] to study the growth of the layer with time. A transfer at a constant speed was begun immediately

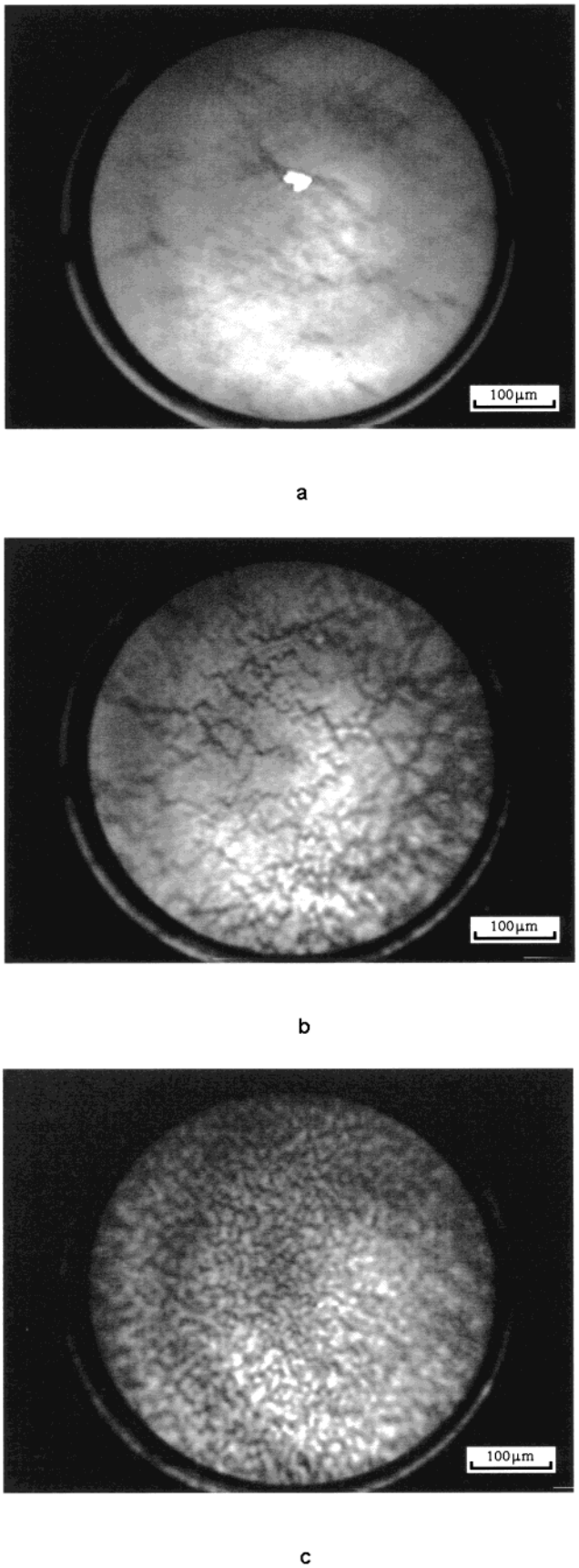

Figure 6. Consecutive BAM images of decompression of a trilayer of fraction TR at 24 °C: (a) immediately after beginning of the decompression; (b) 1 s later; (c) 3 s later.

after compression and continued as the monolayer collapsed. Thus, distances from the dipping line along the substrate

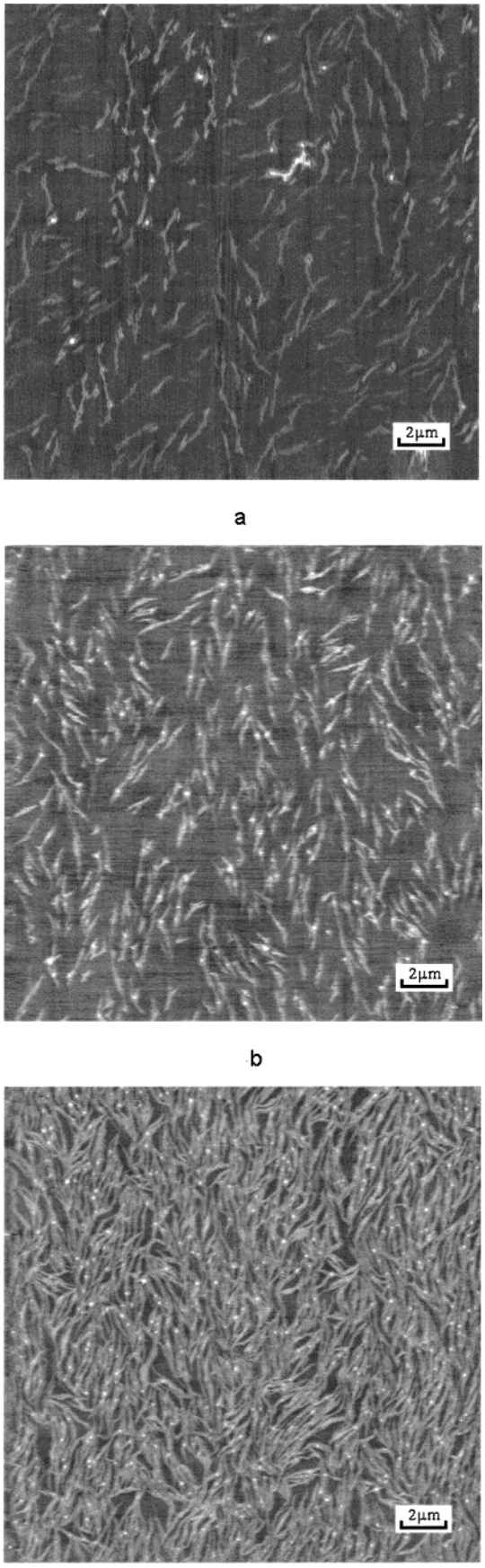

Figure 7. Topographic images of films of fraction II transferred onto mica in the monolayer−bilayer transition region: (a) transfer from point 2 on the isotherm; (b) from point 5; (c) from point 6.

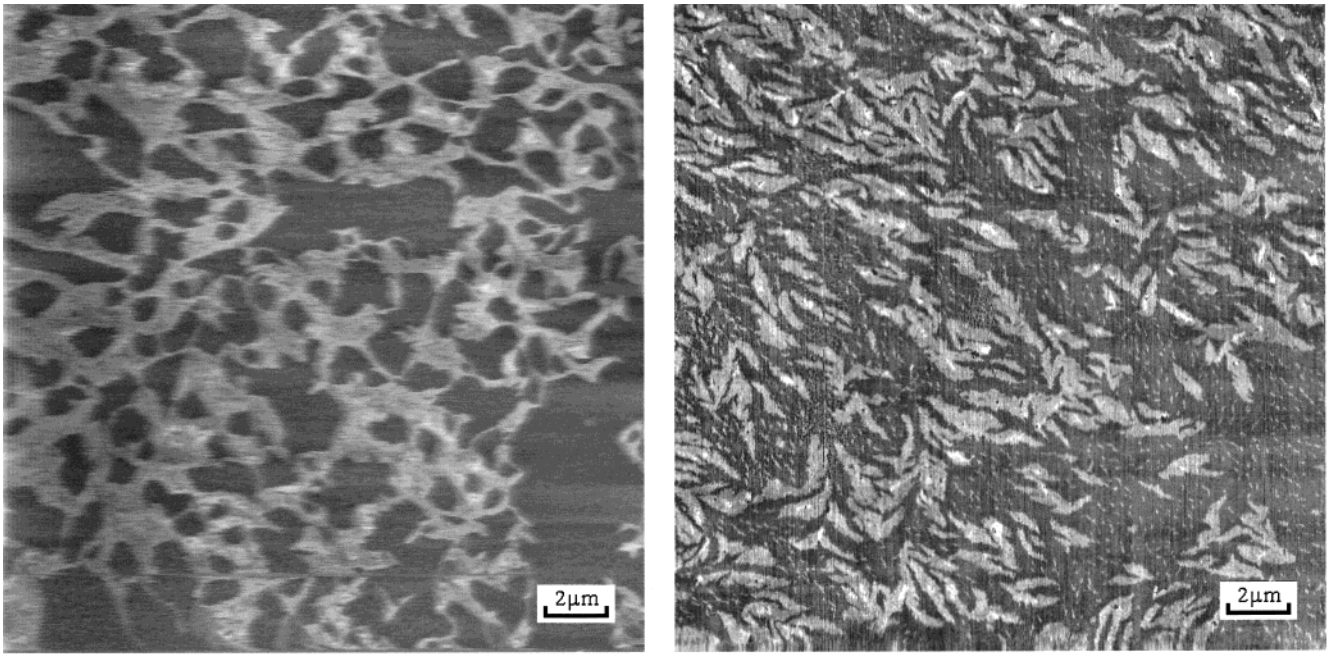

Figure 8. Topographic images of films transferred onto mica in the monolayer−bilayer transition region: (a) fraction I transferred from point 5; (b) fraction IV, point 5.

represent different times after the intiation of collapse and SFM scans made at different places along the substrate provide images of the surface layer as it evolves in time.

Figure 9 shows three regions from the same transfer of fraction I. They were 250 μm apart on the substrate, which for a dipping speed of 0.5 mm min^{-1} corresponds to an interval of 30 s between images. Formation of the second layer begins at places where there are surface defects. We observe that ringlike islands three to four layers thick are formed at these points and monolayer-thick ribbons grow from them as the collapse continues. (Shadows on the right side of the surface features in Figure 9a are artifacts of the tip scanning process and have no physical significance.) Similar behavior was also observed for fractions II and III and for methyl-substituted polymers.[18] However, the ringlike shape of the nucleation centers was found only for fraction I. No bilayer ribbons were observed at the collapse point for the high-molecular-weight fractions IV and V.

The width of the ribbons at the collapse point was 45 ± 10 nm for fraction I and 55 ± 10 nm for fraction II, about one-quarter the width observed for the same fraction in transfers from plateau region C. This difference is likely the result of the different conditions of bilayer formation. In the case of transfers from the collapse point, the monolayer is compressed to a surface pressure higher than the equilibrium spreading pressure, but lower than the dynamic surface pressure of the plateau. The conditions are therefore closer to equilibrium than those in transfers from the plateau, when the layer is quickly compressed until the transfer point. This suggests that the width of the ribbons might depend on the rate of compression. No difference in the ribbon width was observed, however, when the compression rate was 6 times higher.

Specific Features of the Trans-Tactic Polymer. AFM images from different stages of bilayer formation of the trans-tactic fraction TR are shown in Figure 10. The morphology of the bilayer in the low-molecular-weight trans-tactic fraction is markedly different from those obtained with the atactic polymers. The second layer is made up of short ribbons. The density of ribbons is quite uniform throughout the bilayer, but they are organized into regions with characteristic dimensions of about 10 μm in which the chains are parallel and there are relatively sharp boundaries between the regions of different chain orientation. In the later stages of compression, patches of continuous bilayer appear, Figure 10b, that correspond to the bright spots seen in the BAM images in Figure 5; the ribbons are too small to be resolved by the BAM. The size of the patches increases with compression and the ribbons appear to branch, Figure 10c.

Discussion

The most striking feature in experiments is the formation of the bilayer ribbons, which we believe is associated with the collapse process. This conclusion rests, of course, on the assumption that the structure of the collapsing monolayer is unaltered by the transfer to the mica support. Since the ribbons are too narrow to be resolved by BAM, we are unable to demonstrate unequivocally that they were present before transfer. We have seen, however, that the larger structures in the BAM images correspond well to the structures seen with SFM, that the relative amounts of monolayer and bilayer in the transferred films are consistent with the isotherm areas, and that the thicknesses of the transferred layers are in reasonable agreement with those calculated from the molecular modeling. Moreover, in earlier SFM studies of collapsing monolayers of 8CB transferred to mica,[12] in which there is a different morphology, we found excellent agreement with BAM measurements; concurrent scanning surface potential measurements on the transferred films showed that the molecular arrangement of the trilayers that are formed is that deduced from studies on floating monolayers. While these results do not prove that the ribbons are associated with collapse on the water surface, they lend support to this assumption.

The origin of the ribbon textures found for the three lower-molecular-weight fractions of the atactic polymer and observed earlier[18] for the methyl-substituted polymer is unclear. What is

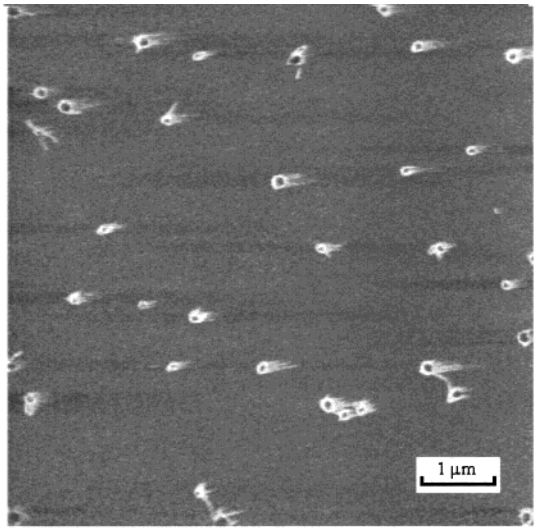

a

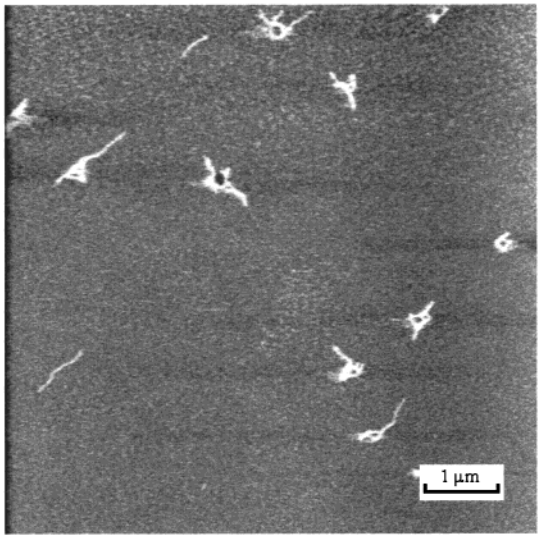

b

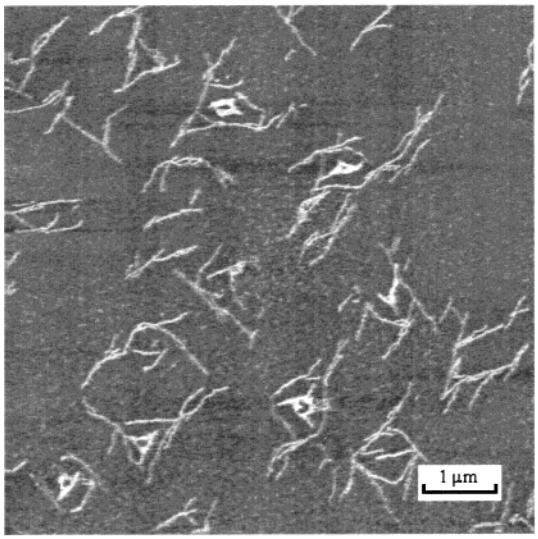

c

Figure 9. Topographic images of a collapsed monolayer of fraction I transferred onto mica from point 2: (a) immediately below the dipping line; (b) 250 μm below the dipping line; (c) 500 μm below the dipping line. The distances correspond to 30 s between images.

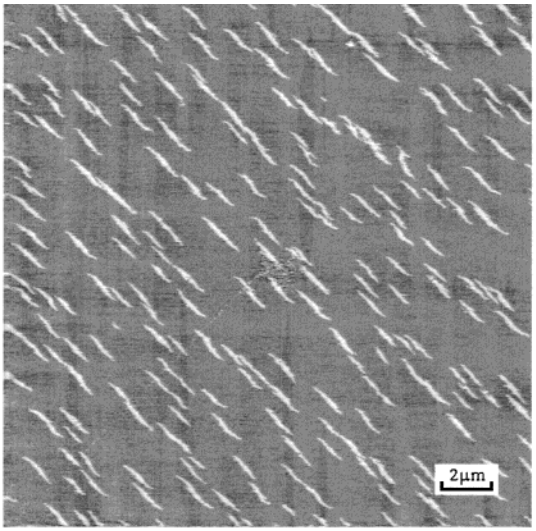

a

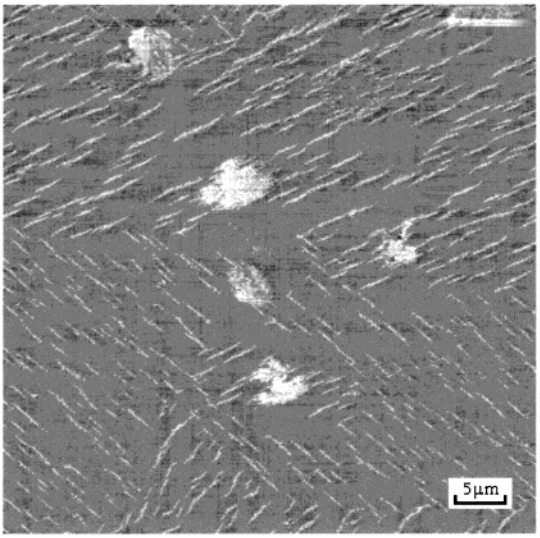

b

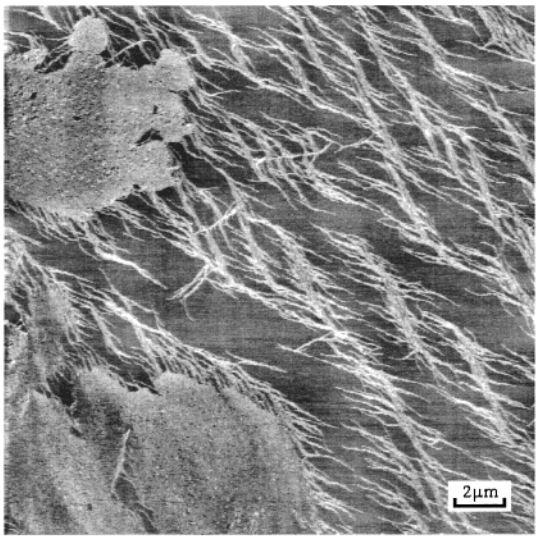

c

Figure 10. Topographic images of of films of fraction TR transferred onto mica in the monolayer−bilayer transition region: (a) point 2; (b) point 3; (c) point 5.

their structure and what controls their width? Ribbons 50 nm wide were observed in *monolayers* of methyl-substituted polymer transferred just below the monolayer-to-bilayer plateau and 200 nm wide ribbons were observed in bilayers at the start of the plateau. In transfers made within the plateau, the width was 500 nm. LFM images of the ribbons in the bilayer displayed a high degree of anisotropy. Ribbons parallel to the scan direction exhibit a higher frictional force than those oriented perpendicular to it. This anisotropy was interpreted as arising from the orientation of the polymer chains perpendicular to the ribbon direction. We have not observed anisotropy in the ribbons of the phenyl-substituted polymer.

All the CLPOS investigated have mesophases[29] in which the chains have an extended conformation.[30] Similar chain conformations have been observed for the mesophase of linear poly(diethylsiloxane) (PDES) for which transmission electron microscopy[31,32] and SFM[33] show a lamellar structure. The width of the lamellae is in good agreement with estimates of the length of an extended chain. Lamellae with two different widths are found in samples with a bimodal molecular weight distribution.[31] Similarly, small-angle neutron scattering studies of the mesophase of poly(dialkylphosphazene)[34] show that the chains are extended.

The persistence length of the atactic polymers is 4.0 nm in the bulk[21] (Kuhn segment length 8.0 nm), so the chains are relatively stiff. Moreover, amphiphiles are necessarily dipolar and when they are spread on the water surface the vertical components of the dipoles have the same orientation, which must lead to a repulsion that will tend to stretch the chains. Thus, it is reasonable to assume that the chains have an extended conformation. One might then expect that the widths of the ribbons would depend on the molecular weights of the polymers. But the results of this study show that this is not so.

In all cases the widths of the ribbons found within the bilayers of the phenyl-substituted polymers are greater than the length of a single extended polymer chain. For example, the degree of polymerization for polymer fraction II is $\bar{x}_n = 35$ and the length of the monomer unit is approximately 1 nm, so a fully extended chain is about 35 nm in length, only about one-sixth of the width of a ribbon formed in the plateau region. Similarly, the widths of the ribbons in bilayers of the methyl-substituted polymer, for which $\bar{x}_n \approx 100$, are about 5 times the length of an extended chain. The narrowest ribbons that we have observed, at the collapse point for the phenyl-substituted polymers and in monolayers of the methyl-substituted polymers, are about 50 nm in width, 2−3 times the length of an extended chain.

The insensitivity of the ribbon width to the molecular weight suggests that the polymer chains may be parallel to the ribbon direction rather than perpendicular to it. Our earlier interpretation of the origin of the anisotropy in the LFM images of methyl-substituted polymer may have been naive; the origin of frictional force differences is not always obvious.[35] If the chains were parallel to the ribbon direction, then the ribbons would range from 50 to 250 chains wide in the phenyl-substituted polymer and 50 to 500 chains wide in the methyl-substituted monolayer and bilayer. While the differences in behavior between the plateau and the collapse point suggest that the kinetics of growth plays a role in determining the width, it seems less likely that the minimum width of 50 nm, which was found in both a monolayer and bilayer, is determined by kinetics.

At the start of the plateau region, the ribbons in the trans-tactic polymer bilayers are much shorter than those in the atactic polymers. Upon closer examination, however, it can be seen that they are composed of segments of short ribbons 100 nm wide. Fine ribbons are apparent in the image made at higher density (Figure 8c); they appear to have grown laterally from the initial short segments.

The pattern of regions containing parallel chains of similar size but different orientations suggests that the trans-tactic bilayer nucleates randomly on the surface. The regularity of the organization within each region probably reflects the underlying regular organization of the phenyl groups in the monolayer, which is absent in the atactic polymers. The orientation of the second layer with its phenyl groups down would lead to what is essentially epitaxial growth.

Monolayer ribbon textures are not unique to the polymeric systems that we have studied. Ribbons 80 nm wide and 100 μm long have been in AFM studies of monolayers of 4-heptoxy-4′-carboxyazobenzene transferred to mica.[36] When droplets of a dilute solution of a peptide oligomer are adsorbed on mica, either from solution or by allowing droplets to dry on the mica surface, long monolayer ribbons are produced.[37] The formation of ribbons may therefore be a general phenomenon not associated with the polymeric nature of the systems that we have studied.

Ribbonlike textures are also found in monolayers of simple amphiphiles, in which case they are attributed to a balance between line tension and the repulsive forces between the vertical components of the molecular dipole moments of the amphiphiles, which are aligned by the water surface.[38] Some numerical estimates show that this mechanism might apply as well to the ribbon textures that we have observed.

McConnell and Moy[39] have shown that circular monolayer domains can undergo a shape transition to an elongated structure when the radius exceeds a critical value R_C. The controlling factor is the ratio of the line tension of the domain λ to the square of the dipole-moment density μ:

$$R_C = \frac{e^{10/3}\delta}{4} e^{\lambda/\mu^2} \tag{1}$$

The parameter δ is the characteristic size of a dipolar unit, which we will take as a monomer. As the domains continue to grow, they can form stripes, whose width is[38,39]

$$w = 2e\delta e^{\lambda/\mu^2} \tag{2}$$

The dipole moment density can be obtained from measurements of the surface potential difference ΔV between the domain and its surroundings. Mann et al.[4] have shown that ΔV can be used directly in the exponential

$$w \approx 2e\delta e^{2n\lambda/\epsilon_0(\Delta V)^2} \tag{3}$$

Surface potential studies of the methyl-substituted polymer[23] show $\Delta V = 200$ mV in the monolayer−bilayer plateau. If we take $w = 50$ nm and $\delta = 1$ nm, we find $\lambda \approx 10^{-13}$ N. This value for the line tension is 2 orders of magnitude smaller than that found for condensed monolayer domains of small amphiphiles (except in the neighborhood of a critical point[40]), but it is in good agreement with line tensions in polymer monolayers.[4,41] From eqs 1 and 2 we obtain $R_C = 1.3w = 65$ nm. This is about the size of the droplets observed in the early stages of collapse, Figure 9, and the subsequent growth of ribbons from them is consistent with their instability. The absence of ribbons in the higher molecular weight polymers might then be attributable to higher line tensions, which would lead to larger critical radii. It has been observed[42] that the surface tension of polymer melts varies as $M_W^{-2/3}$. If this were the case for the

line tension as well, the critical radii for polymer fractions IV and V would be 2−3 orders of magnitude larger than that for fraction I, consistent with the absence of stripes. However, if the molecular-weight dependence of the line tension were this strong we would expect the critical radius and stripe width for polymer fraction III to be 15 times larger than those for fraction I, which is not observed. We conclude that there is some evidence that the balance between dipolar interactions and line tension plays a role in the formation of the stripes; it is not clear, however, that this is the only mechanism.

Acknowledgment. The research described in this publication was made possible in part by Award No. RC1-210 of the U.S. Civilian Research & Development Foundation for the Independent States of the Former Soviet Union (CRDF) and by support of the National Science Foundation (Grant CHE 97-08472) and the Russian Foundation for Basic Research (Grant 99-03-3351) and INTAS (Grant 97-0485). Yu.K.G. is also grateful to the Alexander von Humboldt Foundation for a research award. We thank Professor K. N. Houk for helpful discussions about the molecular conformations.

Note Added in Proof. Mann et al., in a paper subsequent to ref 4 (Mann, E. K.; Hénon, S.; Langevin, D.; Meunier, J.; Leger, L. *Phys. Rev.* **1995**, *51*, 5708) report that the line tension of condensed domains in Langmuir monolayers of poly(dimethylsiloxane) is 1.1 ± 0.3 pN, rather than 0.1 pN.

References and Notes

(1) See, e.g.: Fox, W.; Taylor, P. W.; Zisman, W. A. *Ind. Eng. Chem.* **1947**, *59*, 1401. Gaines, G. L., Jr. *Langmuir* **1991**, *7*, 834. Gaines, G. L., Jr. *Insoluble Monolayers at Liquid−Gas Interfaces*; Wiley-Interscience: New York, 1966; p 172.
(2) Hénon, S.; Meunier, J. *Rev. Sci. Instrum.* **1991**, *62*, 936.
(3) Hönig, D.; Möbius, D. *J. Phys. Chem.* **1991** *95*, 4590.
(4) Mann, E. K.; Hénon, S.; Langevin, D.; Meunier, J. *J. Phys. II Fr.* **1992**, *2*, 1683.
(5) Li, S.; Hanley, S.; Khan, I.; Varshney, S. K.; Eisenberg, A.; Lennox, R. B. *Langmuir* **1993**, *9*, 2243.
(6) See, e.g.: Saito, W.; Mori, O.; Ikeo, Y.; Kawaguchi, M.; Imae, T.; Kato, T. *Macromolecules* **1995**, *28*, 7945.
(7) Rapp, B.; Gruler, H. *Phys. Rev. A* **1990**, *42*, 2215.
(8) Rapp, B.; Eberhardt, M.; Gruler, H. *Macromol. Chem. Macromol. Symp.* **1991**, *46*, 439.
(9) Xue, J.; Jung, C. S.; Kim, M. W. *Phys. Rev. Lett.* **1992**, *69*, 474.
(10) Friedenberg, M. C.; Fuller, G. G.; Frank, C. W.; Robertson, C. R. *Langmuir* **1994**, *10*, 1251.
(11) de Mul, M. N. G.; Mann, J. A. *Langmuir* **1994**, *10*, 2311.
(12) Fang, J. Y.; Knobler, C. M.; Yokoyama, H. *Physica A* **1997**, *244*, 91.
(13) Ibn-Elhaj, M.; Riegler, H.; Möhwald, H. *J. Phys. I Fr.* **1996**, *6*, 969.
(14) Ibn-Elhaj, M.; Möhwald, H.; Cherkaoui, M. Z.; Zniber, R. *Langmuir* **1998**, *14*, 504.
(15) Sheiko, S. S.; Buzin, A. I.; Muzafarov, A. M.; Rebrov, E. A.; Getmanova, E. V. *Langmuir* **1998**, *14*, 7468.
(16) Sautter, E.; Belousov, S. I.; Pechhold, W.; Makarova, N. N.; Godovsky, Yu. K. *Polym. Sci. A* **1996**, *38*, 39.
(17) Belousov, S. I.; Buzin, A. I.; Godovsky, Yu. K. *Polym. Sci. B* **1999**, *41*, N10.
(18) Fang, J.; Dennin, M.; Knobler, C. M.; Godovsky, Yu. K.; Makarova, N. N.; Yokoyama, H. *J. Phys. Chem. B* **1997**, *101*, 3147.
(19) Buzin, A. I.; Sautter, E.; Godovsky, Yu. K.; Makarova, N. N.; Pechhold, W. *Colloid Polym. Sci.* **1998**, *276*, 1078.
(20) Buzin, A. I.; Sautter, E.; Godovsky, Yu. K.; Makarova, N. N.; Pechhold, W. *Polym. Sci. A* **1998**, *40*, 43.
(21) Makarova, N. N.; Godovsky, Yu. K.; Lavrukhin, B. D. *Polym. Sci. A* **1995**, *37*, 225.
(22) Fischer, B.; Tsao, M.-W.; Ruiz-Garcia, J.; Fischer, T. M.; Schwartz, D. K.; Knobler, C. M. *J. Phys. Chem.* **1994**, *98*, 7430.
(23) Belousov, S. I.; Sautter, E.; Pechhold, W.; Makarova, N. N.; Godovsky, Yu. K. *Polym. Sci. A* **1996**, *38*, 1013.
(24) Allinger, N. L. *J. Am. Chem. Soc.* **1977**, *99*, 8127.
(25) Mohamadi, F.; Richards, N. G. J.; Liskamp, W. C.; Lipton, M.; Canfield, C.; Chang, G.; Hendrickson, T.; Still, W. C. *J. Comput. Chem.* **1990**, *11*, 440.
(26) Jorgensen, W. L.; Chandrasekhar, J.; Madura, J. D.; Impey, R. W.; Klein, M. L. *J. Chem. Phys.* **1983**, *79*, 926.
(27) Granick, S.; Clarson, S. J.; Formoy, T. R.; Semlyen, J. A. *Polymer* **1985**, *26*, 925.
(28) Adams, J.; Buske, A.; Duran, R. S. *Macromolecules* **1993**, *26*, 6, 2871.
(29) Godovsky, Yu. K.; Papkov, V. S. *Adv. Polym. Sci.* **1989**, *88*, 129.
(30) Magono, S. N.; Godovsky, Yu. K. Manuscript in preparation.
(31) Molenberg, A.; Möller, M.; Sautter, E. *Prog. Polym. Sci.* **1997**, *22*, 1133.
(32) Magonov, S. N.; Elings, V.; Papkov, V. S. *Polymer* **1997**, *38*, 297.
(33) Molenberg, A.; Möller, M. *Macromolecules* **1997**, *30*, 8332.
(34) Sautter, E. Habilitationsschrift, Universität Ulm, 1997.
(35) See, e.g.: Gehlert, U.; Fang, J.; Knobler, C. M. *J. Phys. Chem. B* **1998**, *102*, 2614.
(36) Sahn, M.; Kamino, A.; Shinkai, S. *Langmuir* **1992**, *8*, 13.
(37) Agelli, M.; Whitehouse, C.; Boden, N.; Fang, J.; Knobler, C. M. Unpublished.
(38) McConnell, H. M. *Annu. Rev. Phys. Chem.* **1991**, *42*, 171.
(39) McConnell, H. M.; Moy, V. T. *J. Phys. Chem.* **1988**, *92*, 4520.
(40) Benvegnu, D. J.; McConnell, H. M. *J. Phys. Chem.* **1992**, *96*, 6820.
(41) Roberts, M. J.; Teer, E. J.; Duran, R. S. *J. Phys. Chem. B* **1997**, *101*, 5647.
(42) Dee, G. T.; Sauer, B. B. *Adv. Phys.* **1998**, *47*, 161.